https://doi.org/10.17221/323/2025-PSE

Greenhouse gas emissions from alluvial soils in grassland and cropland in northern part of Europe's temperate climate zone (Latvia)

Raitis Normunds Meļņiks[1], Arta Bārdule[1], Oleh Prysiazhniuk[2], Oksana Maliarenko[1,2], Inga Jansone[3], Sanita Zute[3], Aldis Butlers[1], Andis Lazdiņš[1]*

[1]*Latvian State Forest Research Institute "Silava", Salaspils, Latvia*
[2]*Institute of Bioenergy Crops and Sugar Beet NAAS, Kyiv, Ukraine*
[3]*Institute of Agricultural Recourses and Economics, Priekuļi, Priekuļu Pagasts, Cēsu Novads, Latvia*
**Corresponding author: raitis.melniks@silava.lv*

Citation: Meļņiks R.N., Bārdule A., Prysiazhniuk O., Maliarenko O., Jansone I., Zute S., Butlers A., Lazdiņš A. (2026): Greenhouse gas emissions from alluvial soils in grassland and cropland in northern part of Europe's temperate climate zone (Latvia). Plant Soil Environ., 72: 194–209.

Abstract: Alluvial soils have high importance for both agriculture and biodiversity; however, these soils can also contribute to greenhouse gas (GHG) emissions including carbon dioxide (CO_2), nitrous oxide (N_2O) and methane (CH_4). In this study, we examined GHG fluxes of three grassland and two cropland sites with alluvial soils in Abava river floodplain, Latvia (Europe). Soil CO_2 fluxes representing heterotrophic respiration (R_{het}) were determined using a portable CO_2 gas analyser, while ecosystem respiration (R_{eco}), soil CH_4 and N_2O fluxes were quantified using a manual closed chamber method combined with gas chromatography. Most alluvial soils acted as source of GHG emissions with the exception of two grassland site where annual CH_4 exchange reflected a slight CH_4 removal from the atmosphere. Mean total GHG emissions (sum of net CO_2, CH_4 and N_2O) were 7.0 ± 3.3 t CO_2 eq./ha/year in grassland sites and 14.5 ± 4.8 t CO_2 eq./ha/year in cropland sites. Net CO_2 contributed the most to total annual GHG emissions with mean values of 6.2 ± 3.3 t CO_2/ha/year in grassland and 13.6 ± 4.8 t CO_2/ha/year in cropland sites. Although the number of study sites is limited, the results support that, in the context of climate change mitigation, grassland represents a more climate-friendly type of floodplain land use than cropland in the hemiboreal region.

Keywords: agricultural alluvial soils; organic matter; flooding-drying conditions; pasture

Alluvium, the parent material of alluvial soils, stands for the unconsolidated sediments deposited by rivers, streams and other fluvial systems (Thorp 1968, Boettinger 2005). Alluvial soils can vary in composition and texture, and they may also contain a large amount of organic matter (OM), thus even corresponding to the organic soil definition set by the Intergovernmental Panel on Climate Change (IPCC) (IPCC 2006). Floodplains with alluvial soils are considered among the most valuable ecosystems due to their capacity to provide specific ecosystem services (Petsch et al. 2023). Alluvial soils are of high importance for agricultural landscapes due to their high potential fertility and productivity (Boettinger 2005). They are also significant for biodiversity due to their moisture dynamic and high value for multiple species and habitats (Šeffer et al. 2008, Kabala 2022) as highlighted under the European Union (EU) Habitats Directive (European Union 1992) and the recently adopted Nature Restoration Law (European Union 2024). Therefore, the sustainable management of floodplains with alluvial soils should aim to balance

Supported by the Latvian State Forest Research Institute "Silava", Projects No. 24-00-S0INZ03-000026 and No. 6.1.1.2/1/25/A/001.

https://doi.org/10.17221/323/2025-PSE

the interests of nature conservation and ecological restoration, as well as the needs of landowners and managers (Donath et al. 2015, Kobierski et al. 2025).

In general, organic soils used for agriculture are a significant contributor to greenhouse gas (GHG) emission profile of many countries. In Latvia, drained organic soils represent a minor part of the total area of agricultural lands (5.77% in cropland and 8.32% in grassland in 2021); however, these soils are responsible for the majority of the total GHG emissions reported in cropland and grassland categories under the Land Use, Land-Use Change and Forestry (LULUCF) sector (Latvia's National Inventory Report 2025). Considering the potential of alluvial soils to store significant amounts of OM, they can also be a source of emissions of the primary GHGs, including carbon dioxide (CO_2), methane (CH_4) and nitrous oxide (N_2O) (Oertel et al. 2016). Furthermore, over a 100-year time horizon, CH_4 and N_2O are 28 and 265 times more potent, respectively, at warming than CO_2 (Myhre et al. 2013). In addition to climatic factors and agricultural activities affecting both the vegetation growth and soil environment (Chataut et al. 2023, Basheer et al. 2024), alluvial soils in river floodplains are affected by periodic or intermittent accumulation of water (Lin et al. 2022). This makes the dynamics of biogeochemical activities and GHG exchange even more complex (Jansson and Hofmockel 2019). Furthermore, several climate change scenarios have projected that heavy precipitation may lead to extended periods of flooding and alternating wet and dry conditions (Tabari 2020, Guo et al. 2023). Sediments subject to drier conditions are active areas for GHG emissions, and higher GHG emissions at transitional dry-wet phases have been observed, showing water level (WL) fluctuation effect (dos Santos Pinto et al. 2020). These changes in soil moisture, caused by prolonged flooding and alternating flooding-drying conditions, can further influence the magnitude of GHG fluxes, with potentially differing impacts on cropland and grassland (Guo et al. 2023). In general, the knowledge on the magnitude of GHG fluxes, including the effect of flooding-drying conditions on biogeochemical cycling in river floodplains is still incomplete (Petsch et al. 2023).

Management strategies of agricultural soils have to balance GHG emission mitigation, soil organic carbon (C) stock preservation and land use productivity (Freeman et al. 2022). The contribution of managed, periodically flooded alluvial soils to Latvia's GHG emission profile of LULUCF sector remains unclear. According to the soil maps of Latvian agricultural land, historically compiled from 1959 to 1991, at a scale of 1:10 00, the total area of alluvial soils is 100 250 ha (Ministry of Agriculture 2019). Improving knowledge of GHG exchange from alluvial soils can contribute to more effective management of these soils, ensuring sustainable agricultural practices, environmental protection and climate change mitigation, considering climate extremes and their implications for zero net GHG emission ambitions (Guo et al. 2023). This study is focused on managed alluvial soils, used as grassland and cropland, in the Abava river valley, Latvia (northern part of Europe's temperate climate zone). The study aims to (*i*) characterise the physico-chemical properties of alluvial soils; (*ii*) estimate the variation in magnitude of CO_2, CH_4, N_2O fluxes and identify the driving forces of these fluxes. We hypothesised that less intensive use of agricultural alluvial soils (grassland) results in lower GHG emissions and higher soil organic C and total nitrogen stocks compared with more intensive use (cropland).

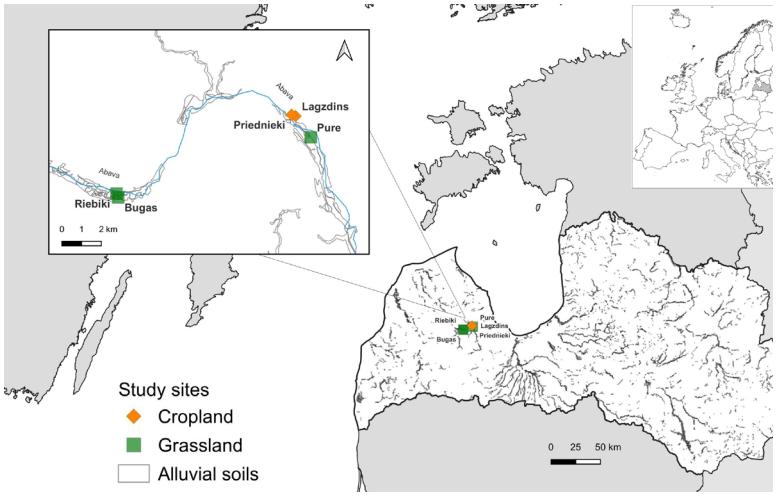

Figure 1. Locations of the study sites in the Abava river valley in Latvia, northern part of Europe's temperate climate zone

https://doi.org/10.17221/323/2025-PSE

MATERIAL AND METHDS

Study sites. The study, conducted in 2022–2024 in Abava river valley in Latvia, investigated two cropland sites and three grassland sites with alluvial soils (Fluvisols) (Figure 1, Table 1). In each study site, three plots with different distances and surface heights above sea level (a.s.l.) were established in

Table 1. General description of the study sites

Type of land use (study site): vegetation	General description	Plot	Coordinates (LKS-92)	Elevation (m a.s.l.)
Grassland (Pūre): grass mixture	**Land use, management and area of study site** – grazed and mown for hay/silage, 2.6 ha (the total area of the floodplain ~ 40 ha). **Livestock** – up to 50 dairy cows are raised under conventional farming by rotating them through 3–5 ha fenced pasture blocks to allow grass regrowth, with 3–4 grazing cycles per season. **History** – ploughed 5–10 years ago. **Vegetation** – dominant graminoids: Cock's-foot *Dactylis glomerata*, *Festuca* spp., *Poa* spp.; near river nettles *Urtica* spp.; farther away graminoids and low broad-leaf herbs (*Taraxacum* spp., *Rumex* spp., *Plantago lanceolata*, *Lotus* spp., *Trifolium repens*). **Fertilisation** – no application reported	A	X: 57.03858, Y: 22.89830	38.32
		B	X: 57.03800, Y: 22.89762	38.40
		C	X: 57.03833, Y: 22.89789	39.25
Grassland (Bugas): grass mixture	**Land use, management and area of study site** – permanent (continuously grazed) pasture, organic farming, 0.6 ha (the total area of the floodplain ~ 22 ha). **Livestock** – beef cattle (the herd consists of up to 40 beef cattle of various ages). **History** – no additional information. **Vegetation** – ground layer dominated by silverweed *Potentilla anserina*, white clover *T. repens*, bentgrass *Agrostis* spp.; creeping buttercup *Ranunculus repens* in lowest areas; wild grasses on slightly higher ground. **Fertilisation** – no application reported	A	X: 57.00969, Y: 22.73852	33.86
		B	X: 57.00925, Y: 22.73770	34.37
		C	X: 57.00942, Y: 22.73721	34.51
Grassland (Riebiķi): grass mixture	**Land use, management and area of study site** – low-intensively managed hayfield (1 harvest/year), organic farming, 0.82 ha. **History** – former Abava river channel; uneven micro-relief formed over time. **Vegetation** – depressions: meadowsweet *Filipendula ulmaria*, valerian *Valeriana officinalis*, herb-robert *Geranium robertianum*; ridges: wild grasses plus *Galium verum*, *Ranunculus* spp., *Leontodon* spp. **Fertilisation** – no application reported.	A	X: 57.01146, Y: 22.73703	34.40
		B	X: 57.01195, Y: 22.73743	34.50
		C	X: 57.01155, Y: 22.73657	34.74
Cropland (Priednieki): winter wheat in 2023, red clover in 2024	**Land use, management and area of study site** – arable field, conventional tillage, 0.77 ha. **History** – winter wheat was sown in late September 2022, wheat showed stunted growth in dry 2023, harvested in the first decade of August 2023, stubble left over winter 2023–2024; red clover was sown in June 2024 following spring disc harrow; first-year red clover had not yet been harvested. **Fertilisation** – no application in 2023 and 2024. **Yield** – wheat 2.4 ± 0.5 t/ha (14% moisture content)	A	X: 57.04867, Y: 22.88197	39.20
		B	X: 57.04886, Y: 22.88198	39.50
		C	X: 57.04908, Y: 22.88177	39.92
Cropland (Lagzdiņš): winter rape in 2023, winter wheat in 2024	**Land use, management and area of study site** – arable field, conventional tillage, 4.65 ha **History** – winter rape was sown in mid-August 2022, harvested in the third decade of July; winter wheat was sown in late September 2023, harvested in the first decade of August 2024. **Fertilisation** – **2023:** 300 kg/ha ammonium sulfate (N21S24, 14 April 2023), 200 kg/ha nitrogen (N33, 21 April 2023); **2024:** 300 kg/ha ammonium sulfate (N21S24, 3 April 2024), 200 kg/ha nitrogen (N33, 28 April 2024). **Yield** – rapeseed 6.5 ± 0.9 t/ha (8% moisture content); wheat 2.1 ± 0.1 t/ha (14% moisture content).	A	X: 57.04809, Y: 22.88528	39.72
		B	X: 57.04798, Y: 22.88641	40.11
		C	X: 57.04784, Y: 22.88624	40.61

https://doi.org/10.17221/323/2025-PSE

Table 2. General description of meteorological conditions in Latvia and in the study area (LEGMC 2024)

Parameter	Long-term average				Study period			
	1991–2020		2022		2023		2024	
	Latvia	study area*	Latvia	study area*	Latvia	study area*	Latvia	study area*
Mean annual precipitation (mm)	686	696	686	656	761	721	654	618
Mean annual air temperature (°C)	6.8	6.8	7.3	7.4	7.8	7.7	8.7	8.6

*The nearest meteorological station, "Stende" 15–20 km from study sites, SLLC "Latvian Environment, Geology and Meteorology Centre (LEGMC)"

a transect for GHG flux measurements (Table 1). During the study period, the mean annual precipitation in the study area was slightly lower than the national historical average for Latvia, by approximately 30–40 mm; the difference in mean annual air temperature between the study area and the national average did not exceed 0.1 °C (Table 2).

Floodplain hydrological regime. To determine the flooding period and frequency at the plot level, we combined field observations, hydrological data (water level and discharge) and LGIA (Latvian Geospatial Information Agency) DEM (digital elevation model) analysis (LGIA 2025). During field visits, plots were classified as flooded when access or measurement was prevented by inundation. Daily WLs between visits were estimated using hourly data from the Renda hydrological station (LEGMC), located 35 km downstream. Because of distance from the station and river cross section differences, station levels in river in the locations of each plot were estimated using local river cross-sections derived from a high-resolution DEM and Manning's equation (Arcement and Schneider 1989). DEM data also provided plot elevations along transects from river edge to higher ground. Based on estimated daily WLs, deviations from the 3-year mean, and plot elevations, we calculated the number of inundated days per plot.

Flooding frequency during the study period varied across sites (Table 3). No flooding occurred between April–December 2022. In 2023, flooding was the most frequent at Bugas (plot A, 33 days) and Pure (plots A and B, 30 and 28 days), with peak levels of 2.30–3.64 m above the Renda base level. In 2024, flooding was less frequent, with Bugas plot A again most affected (15 days), and minimal flooding at Pure C and Riebiki C (1 day). Cropland sites Priednieki and Lagzdins remained unflooded throughout; among plots, max WL ranged from –0.25 to –0.97 m and from –0.77 to –1.66 m below plot surface level, respectively.

Measurement of soil heterotrophic respiration. Soil heterotrophic respiration (R_{het}) represents CO_2 fluxes generated during the decomposition of soil OM (including plant residues and flooding sediments) by soil biota such as microorganisms and soil fauna. Measurements of R_{het} were conducted in three replicates per plot during the daytime using a portable CO_2 gas analyser EGM-5 (PP Systems International, Inc., Amesbury, USA) equipped with

Table 3. Characteristics of the floodplain hydrological regime at the grassland study sites during the two-year period (April 2022–March 2024)

Type of land use	Study site	Sub-plot	Days flooded (days)	Events per year (events)	Mean duration (days)	Max duration (days)	Max water level (m)
Grass-land	Bugas	A	48	3.5	6.9	17	1.19
		B	20	3.0	3.3	6	0.68
		C	12	2.0	3.0	4	0.54
	Pure	A	38	3.5	5.4	16	1.03
		B	35	3.0	5.8	15	0.95
		C	4	1.0	2.0	2	0.09
	Riebiki	A	19	3.0	3.2	6	0.65
		B	13	2.5	2.6	4	0.55
		C	6	1.5	2.0	3	0.30

https://doi.org/10.17221/323/2025-PSE

a SRC-2 soil respiration chamber (volume 1 171 mL, measurement area 78 cm^2). R_{het} measurements were conducted by placing the soil respiration chamber on bare soil (Ojanen et al. 2012, Dyukarev 2017). Each R_{het} measurement point (area) was prepared in advance by cutting aboveground biomass; the further spread and development of vegetation at the R_{het} measurement point were prevented by covering the soil with geotextile between surveys of the study sites. Measurements of CO_2 fluxes were conducted in 2022–2024 at the grassland study sites, and in 2023–2024 at the cropland study sites. Measurements were carried out once every three weeks during the growing season, from April to October.

Gas sampling and analysis. To estimate CO_2 fluxes representing ecosystem respiration (R_{eco}) – the sum of R_{het} from OM decomposition and autotrophic respiration (R_{aut}) of aboveground and belowground plant biomass – as well as CH_4 and N_2O fluxes, gas sampling was conducted once per month from April 2023 to December 2024. In each plot, two permanent circular collars were installed into the soil (extending to a depth of 5 cm) with a 0.5–1 m distance between collars, avoiding vegetation disturbance. Gas sampling was conducted during the day using a manual closed-chamber method (Pavelka et al. 2018). Chambers (non-transparent, volume 0.0655 m^3, diameter 50 cm) were positioned on the collars, and after closing, four consecutive gas samples (50 cm^3) were sampled at 10 min intervals (immediately after positioning the chamber on the collar and then after 10, 20, and 30 min) using underpressurised (30 Pa) glass vials. CO_2, CH_4, and N_2O concentrations in gas samples were determined using the Shimadzu Nexis GC-230 gas chromatograph (Shimadzu USA Manufacturing, Inc., Canby, USA) equipped with an electron capture detector (ECD) and flame ionisation detector (FID) at the Latvian State Forest Research Institute (LSFRI) "Silava" (LVS EN ISO 17025:2018-accredited laboratory). The expanded uncertainty (equal to twice the combined uncertainty) of the method was estimated to be 4.8% for CO_2, 2.3% for CH_4, and 13.0% for N_2O (Magnusson et al. 2017). The estimated cumulative reproducibility of chamber-based gas sampling and analysis is 10% for CO_2 (Butlers et al. 2025).

Estimation of GHG fluxes. GHG fluxes were calculated for each measurement event using the equation of ideal gas law and the slope of the linear regression reflecting the change in GHG concentration in the chamber over the 150-second period of linear concentration increase for R_{het} and over a 30 min period (based on the results of GHG concentrations in four consecutive sampled gas samples) for R_{eco}, CH_4, and N_2O according to the Eq. 1.

$$Instantaneous\ GHG\ flux = \frac{M \times P \times V \times slope}{R \times T \times A} \quad (1)$$

where: Instantaneous GHG flux – instantaneous GHG (CO_2, CH_4 or N_2O) flux (μg GHG/m^2/h); M – molar mass of GHG (g/mol); P – assumption of air pressure inside the chamber (101 300 Pa); V – chamber volume (m^3); *slope* – GHG concentration changes over time (ppm/h); R – universal gas constant (8.314 m^3·Pa/K/mol); T – air temperature (K); A – measurement area (m^2).

Quality control (QC) of the data included evaluating the linearity of changes in GHG concentrations in the gas samples over time within the closed chamber (a detailed description of the QC procedure is provided in Bārdule et al. (2025) and Butlers et al. (2025)).

Measurement of environmental parameters. Soil samples were collected once in the grassland study sites in March 2022 and in the cropland study sites in April 2023. Soil samples were taken to a depth of 80 cm from the following layers: 0–10, 10–20, 20–40 and 40–80 cm. Two sets of soil samples were taken: (*i*) one set for determining soil physical properties, including soil bulk density and soil texture (unmixed soil samples with a volume of 100 cm^3 were taken from the middle of each selected soil layer); (*ii*) the second set for soil chemical analysis (mixed samples were taken from the whole selected soil layer). Soil physico-chemical analyses were performed at the LSFRI "Silava" (LVS EN ISO 17025:2018-accredited laboratory). The following variables were determined: (*i*) soil bulk density (LVS ISO 11272:2017); (*ii*) soil texture or proportion of sand (particle size 2 mm – 63 μm), silt (particle size 63–2 μm) and clay (particle size < 2 μm) particles according to the LVS ISO 11277:2010; (*iii*) soil pH in 1 mol/L potassium chloride (KCl) suspension according to the LVS ISO 10390:2021; (*iv*) total nitrogen (N_{tot}) content using dry combustion (elemental analysis, LVS ISO 13878:1998); (*v*) organic carbon (C_{org}) content calculated as difference between total carbon content (C_{tot}), determined using dry combustion (elementary analysis, LVS ISO 10694:2006), and inorganic C or carbonate content (C_{carb}) determined using digital soil calcimeter; (*vi*) phosphorus (P), potassium (K), calcium (Ca) and magnesium (Mg) content was determined by microwave digestion (concentrated nitric acid extract) and inductively coupled plasma optical emission spectrometry (ICP-OES) method according to the LVS EN ISO 11885:2009.

https://doi.org/10.17221/323/2025-PSE

Simultaneously with GHG flux monitoring, soil temperature (°C) at 7 cm depth and soil moisture (volumetric water content, %) in the 0–7 cm layer were measured using an EGM–5 equipped with a soil moisture and temperature probe (Stevens Hydra Probe soil sensor). At grassland sites, during study site surveys, soil water-table level (WTL) was measured manually using groundwater wells (PVC pipes) installed vertically at 1.5 m depth (one well per plot). In cropland sites, groundwater wells were not installed.

We used meteorological data from the nearest LEGMC station to calculate a set of indirectly measured environmental variables (agro-hydrological and fire-weather indices describing water and moisture conditions), which we included in correlation and PLS (partial least-squares) regression. Reference evapotranspiration (ET_o) was calculated using the FAO-56 Penman-Monteith (Allen et al. 1998) method as a climatic baseline of atmospheric water demand, and actual evapotranspiration (ET_c) was derived by applying land-cover-specific crop coefficients to ET_o. Daily water balance (Q) was computed as the difference between precipitation, ET_c, with moving sums over 7, 30, and 40 days characterising short- to medium-term moisture conditions. Moisture anomalies were quantified using the Standardised Precipitation-Evapotranspiration Index (SPEI) at 7-, 30-, and 60-day timescales (Vicente-Serrano et al. 2010) using the R module SPEI (Beguería et al. 2014). Fire danger was assessed using the Canadian Fire Weather Index (FWI) system (Van Wagner 1987) using the R package *cffdrs* (Wang et al. 2025). The index was initially developed to characterise fire-spread potential, representing surface-to-deep-layer fuel moisture.

Sampling and analysis of aboveground and root biomass. In all study sites, aboveground and root biomass were sampled in 2023 and 2024. The sampling area was 0.125 m^2. The root biomass was sampled by excavating roots down to 20 cm depth. In grassland sites, aboveground biomass was sampled three times per growing season in 2023 and twice per growing season in 2024. Root biomass was sampled only at the end on growing season. At cropland sites, both aboveground and root biomass were sampled during summer, when plant development is at its maximum. At the Priednieki study site in 2024, when red clover was cultivated for the first year, aboveground biomass was sampled three times per growing season, while root biomass was sampled only at the end of the growing season.

All vegetation samples were transported to the laboratory, and their dry mass was determined after drying at 70 °C until a constant mass was reached. Before drying, root biomass samples were separated from soil particles by washing with cold tap water and wet sieving. The C_{tot} content in biomass samples was determined by elementary analysis (LVS ISO 10694:2006).

Estimation of cumulative annual GHG fluxes. Cumulative annual (January–December) GHG fluxes were calculated as a cumulative value of the monthly mean fluxes (expressed as t CO_2-C/ha/month, kg CH_4-C/ha/month, kg N_2O-N ha/month) according to Eq. 2.

$$Cumulative\ annual\ GHG\ flux = \sum_{i=Jan}^{Dec} Monthly\ mean\ GHG\ flux \quad (2)$$

Where: Cumulative annual GHG flux is the annual (January–December) GHG fluxes (t CO_2-C/ha/year, kg CH_4-C/ha/year, kg N_2O-N/ha/year); Monthly mean GHG flux – monthly mean GHG flux in month i (t CO_2-C/ha/month, kg CH_4-C/ha/month, kg N_2O-N/ha/month), i – calendar months from January to December.

Annual net CO_2 fluxes for each study site were calculated as the difference between annual soil R_{het} and C input into soil with plant litter. Annual soil R_{het} was calculated as a cumulative value of the monthly mean fluxes of R_{het} (growing season) and R'_{het} (non-growing season when R_{het} was not measured). R'_{het} was calculated assuming that the proportion of R'_{het} to R_{eco} is 0.62 (Jian et al. 2021) if the air temperature is above 5 °C, while R_{eco} equals R'_{het} if the air temperature is below 5 °C.

For cropland, C input into soil with plant litter was estimated as the sum of C amount in above- and belowground (root) harvest residues. For grassland, it was assumed that the C input into soil with the aboveground parts of vegetation equalled the C stock in aboveground biomass at the end of the growing season. In contrast, the C input into soil with root biomass was calculated assuming a root turnover rate of 0.41 (Palosuo et al. 2015).

Cumulative annual GHG emissions were expressed as CO_2 equivalents (eq.) according to the global warming potential (GWP) values for a 100-year time horizon; GWP values of 1, 28 and 265 were used for CO_2, CH_4 and N_2O, respectively (Myhre et al. 2013).

Statistical analysis. All statistical analyses were performed with licensed Statistica software (Cassell 2016) with additional integrated R modules (pastecs::stat.desc(), Hmisc::rcorr()) and with R (ver-

https://doi.org/10.17221/323/2025-PSE

sion 4.3.3, Vienna, Austria) and RStudio 2023.12.1 (R Core Team 2024). The normality hypothesis and the homogeneity of variance of the experimental data were tested using the Shapiro-Wilk W test and the histogram of the normal distribution. Further statistical processing was performed using non-parametric statistics.

The Wilcoxon rank-sum exact test with pairwise comparisons adjusted for multiple testing using the Bonferroni correction was used to estimate statistically significant differences in soil physicochemical variables and GHG fluxes. To link mean GHG fluxes to various environmental factors, Spearman correlation (ρ) analysis was performed. A significance level of $P < 0.05$ was used.

Partial least squares (PLS) regression, a multivariate method suitable for linearly correlated variables such as environmental variables, was used (R package mdatools, Kucheryavskiy 2020). PLS regression analysis includes the evaluation of X variables (environmental variables) depending on their importance in explaining Y (GHG fluxes), expressed as variables important for the projection (VIP values). X variables with VIP < 0.8 were considered to be insignificant

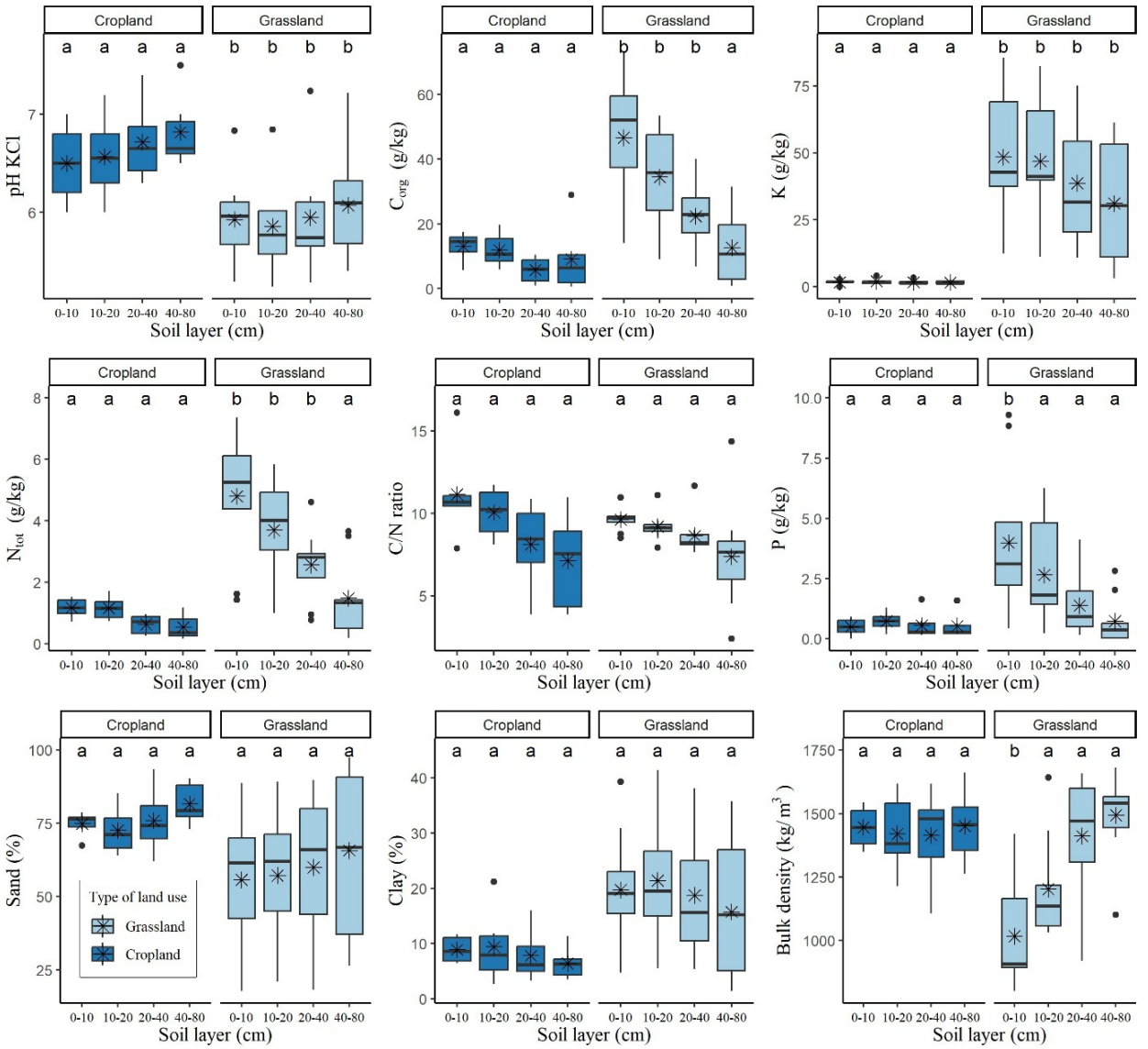

Figure 2. Soil physical and chemical variables in different soil layers in cropland and grassland study sites. In boxplots, medians are shown as bold horizontal lines within the boxes, which indicate the interquartile range from the 25th to the 75th percentiles; the mean values are shown as black asterisks; the minimum and maximum values are shown as whiskers; and outliers are shown as black dots. Statistically significant differences ($P < 0.05$) between cropland and grassland within the soil layer are denoted by the lowercase letters a and b

https://doi.org/10.17221/323/2025-PSE

and were not retained in the PLS regression, while X variables with VIP > 1.0 were considered to be important.

RESULTS AND DISCUSSION

Soil physico-chemical variables. No statistically significant differences in soil physical variables in different soil layers were observed either between individual study sites or between sites grouped by land use type (grassland *vs*. cropland), with the exception of soil bulk density in the 0–10 cm layer, which was significantly higher in the cropland sites compared to the grassland sites ($P = 0.002$, Figure 2). Similarly, no statistically significant differences in the mean soil chemical variables across different soil layers were observed among the individual study sites (Figure 2). When comparing the mean soil chemical variables between study sites grouped by land use type, significantly higher contents of C_{org} and N_{tot} ($P < 0.03$ in soil layers at depths of 0–40 cm), P ($P = 0.02$ in 0–10 cm soil layer), K, Ca and Mg ($P < 0.02$ in soil layers at depths of 0–80 cm) were observed in the grassland study sites, whereas soil pH was significantly higher in the cropland study sites ($P < 0.03$ in soil layers at depths of 0–80 cm). In general, higher C_{org} and N_{tot} were associated with higher levels of the other studied nutrients (P, Ca, K, Mg), as indicated by positive correlations ($\rho > 0.74$; all soil layers pooled). In general, clustering of study sites based on soil physical and chemical variables showed greater similarity among cropland sites, whereas grassland sites showed greater variability in their soil variables.

Although theoretically alluvial soils can store a significant amount of C_{org}, the studied alluvial soils at both grassland and cropland sites in the Abava River valley in Latvia did not meet the IPCC definition of organic soil (IPCC 2006). Thus, the reporting of GHG emissions from these soils is not mandatory in the national GHG inventory. The higher C_{org} content in 0–40 cm soil layer observed in grassland sites (mean 31.5 ± 9.8 g/kg) compared to cropland sites (9.2 ± 3.2 g/kg) can be explained by a combined impact of higher soil C inputs by plant residues and substantial belowground biomass, which contribute continuous rhizodeposits (Tripolskaja et al. 2024, Table 4), reduced soil disturbance (van Eekeren et al. 2025), and

Table 4. A rough estimate of cumulative annual greenhouse gas (GHG) fluxes in the grassland and cropland study sites (mean ± standard error (SE) values shown)

Cumulative annual GHG fluxes	Unit	Land use type and study site						
		grassland				cropland		
		Pūre	Bugas	Riebiķi	mean	Priednieki	Lagzdiņš	mean
R_{het}	(t CO_2-C/ha/year)	7.3 ± 1.1	7.6 ± 1.0	9.2 ± 0.3	**8.1 ± 0.6**	7.6 ± 1.1	5.2 ± 0.4	**6.4 ± 1.2**
Carbon input (plant residues)	(t C/ha/year)	5.1 ± 0.4	6.7 ± 0.7	7.5 ± 0.6	**6.4 ± 0.7**	3.2 ± 0.3	2.2 ± 0.2	**2.7 ± 0.5**
Net CO_2 fluxes	(t CO_2-C/ha/year)	2.2 ± 1.2	0.9 ± 1.2	1.7 ± 0.7	**1.7 ± 0.9**	4.4 ± 1.1	3.0 ± 0.4	**3.7 ± 1.3**
	(t CO_2/ha/year)	8.1 ± 4.3	3.3 ± 4.5	6.2 ± 2.5	**6.2 ± 3.4**	16.1 ± 4.2	11.0 ± 1.6	**13.6 ± 4.8**
CH_4 fluxes	(kg CH_4-C/ha/year)	–0.1 ± 0.9	0.7 ± 0.5	–2.8 ± 0.8	**–0.7 ± 1.1**	0.2 ± 0.5	0.4 ± 1.7	**0.3 ± 0.1**
	(t CO_2 eq./ha/year)	–0.01 ± 0.03	0.03 ± 0.02	–0.10 ± 0.03	**–0.03 ± 0.04**	0.01 ± 0.02	0.02 ± 0.06	**0.01 ± 0.01**
N_2O fluxes	(kg N_2O-N/ha/year)	2.4 ± 0.7	2.1 ± 0.6	1.2 ± 0.7	**1.9 ± 0.4**	2.6 ± 0.6	2.0 ± 0.3	**2.3 ± 0.3**
	(t CO_2 eq./ha/year)	1.0 ± 0.3	0.9 ± 0.3	0.5 ± 0.3	**0.8 ± 0.2**	1.1 ± 0.2	0.8 ± 0.1	**1.0 ± 0.1**
Total net GHG fluxes	(t CO_2 eq./ha/year)	9.1 ± 4.3	4.2 ± 4.5	6.6 ± 2.5	**7.0 ± 3.4**	17.2 ± 4.2	11.8 ± 1.6	**14.5 ± 4.8**

R_{het} – heterotrophic respiration

https://doi.org/10.17221/323/2025-PSE

overall differences in soil texture (Guillaume et al. 2022, Figure 2). Theoretically, additional OM could be transported and deposited during flood events, which were more frequently observed in grassland sites (Table 3). Similar results were reported by Kobierski et al. (2025) in Poland, who found higher soil C_{org} storage in grasslands (10.9 kg/m^2) than in croplands (6.7 kg/m^2) in Vistula river floodplains with Fluvisols, emphasising the role of grassland as soil C_{org} reservoirs.

In the studied grassland sites, the mean C_{org} content in the 0–20 cm soil layer (40.6 ± 9.1 g/kg) was higher than the previously reported mean values for mineral soils in grassland in Latvia by Bardule et al. (2017) (25.1 ± 5.3 g/kg), while falling within the range reported more recently by Petaja et al. (2024) (7.2–46.0 g/kg). Conversely, in the studied cropland sites, the mean C_{org} content in 0–20 cm soil layer (12.6 ± 2.8 g/kg) was lower than the previous estimates for mineral soils in cropland in Latvia (mean of 21.2 ± 3.0 g/kg according to the Bardule et al. (2017) and ranged from 11.8 ± 2.6 g/kg in Arenosols to 19.9 ± 8.7 g/kg in Gleysols according to the Petaja et al. (2024)). However, Fluvisols were not included in these previous studies.

Higher bulk density and a greater proportion of sand particles – variables that were positively intercorrelated (ρ = 0.55, all soil layers pooled) – were associated with relatively lower contents of C_{org}, N_{tot} and other nutrients, showing negative correlations (ρ values ranged from –0.41 to –0.75, all soil layers were pooled). In contrast, the finest soil particles analysed (clay) showed a positive correlation with the contents of C_{org}, N_{tot}, and other nutrients (ρ > 0.67, across all soil layers pooled). In general, fine mineral particles in soil play an important role in binding and increasing the persistence of OM through sorption at the reactive surfaces of minerals and occlusion in aggregates (Schweizer et al. 2021). These interactions between soil OM and soil fine particles reduce soil susceptibility to mineralisation and further release of decomposition products into the atmosphere or through leaching (Schweizer et al. 2021).

The soil C/N ratio, a proxy of the decomposability of soil OM and the potential for N immobilisation or mineralisation (Amorim et al. 2022), was mostly below 12 in the studied sites (ranged from 9.0 to 12.7 in the 0–10 cm soil layer and from 8.5 to 10.2 in the 10–20 cm soil layer). This generally reflects

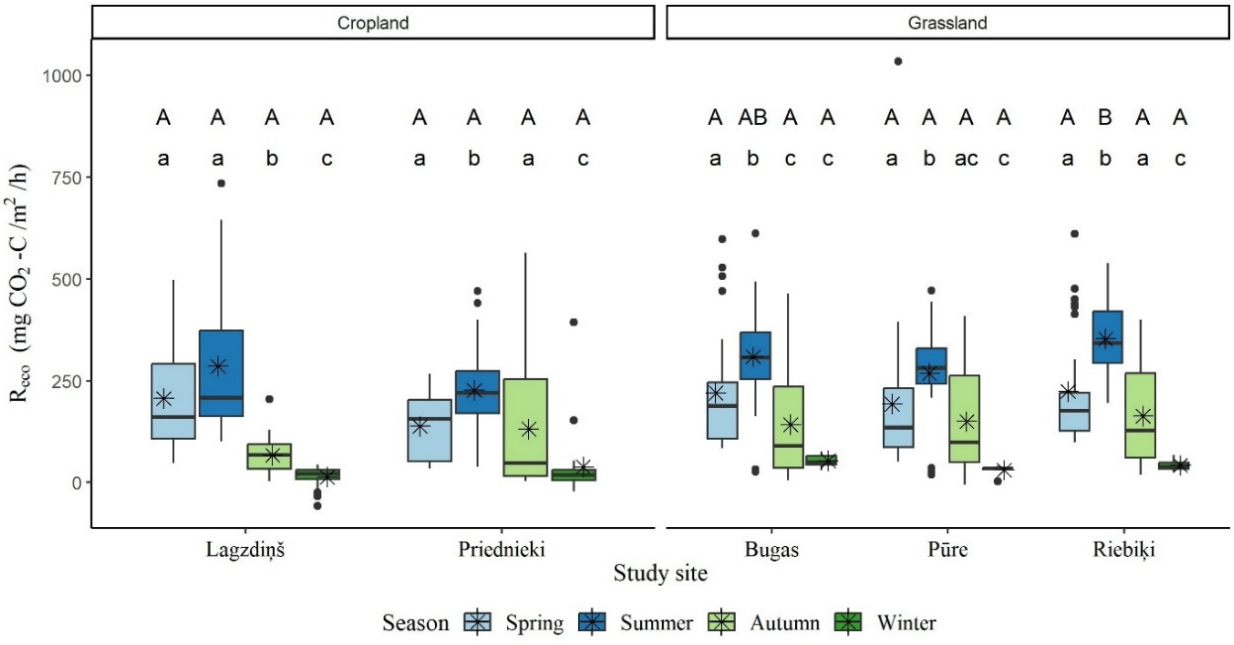

Figure 3. Variation in Reco across different study sites and seasons during the study period. Spring – March, April, May; Summer – June, July, August; Autumn – September, October, November; Winter – December, January, February. In boxplots, medians are shown as bold horizontal lines in the boxes that indicate the interquartile range from 25th to 75th percentiles, the mean values are shown as black asterisks, and outliers are shown as black dots. Statistically significant differences (P < 0.05) between different seasons within the same study site are denoted by the lowercase letters a, b and c; statistically significant differences between different study sites within the same season and land use type are denoted by the uppercase letters A and B

https://doi.org/10.17221/323/2025-PSE

rapid mineralisation of OM and N release, making N potentially available for plant uptake (Brust 2019). In general, the soil C/N ratios obtained in the studied alluvial soils are comparable to those previously reported for Fluvisols in Europe. For instance, grassland Fluvisols along the Lower Vistula floodplain in Poland showed a slightly higher mean C/N ratio (10.4) than adjacent cropland Fluvisols (9.4) (Kobierski et al. 2025).

Variation in GHG fluxes and the affecting factors. Statistically significant differences ($P < 0.05$) in R_{eco} fluxes, which comprise CO_2 fluxes from OM decomposition (R_{het}) as well as from R_{aut} of both aboveground and belowground plant biomass, were observed not only among different seasons within the same study site but also among study sites (Figure 3). Mean R_{eco} fluxes ranged from 13.7 ± 5.4 mg CO_2-C/m^2/h in winter in the cropland site Lagzdiņš (the lowest seasonal mean value among the study sites and seasons) to 353.0 ± 13.6 mg CO_2-C/m^2/h in summer in the grassland site Riebiķi (the highest seasonal mean value). When pooling data by land use type, significantly higher R_{eco} was observed in grassland sites than in cropland sites in summer, autumn and winter ($P < 0.001$). Annual mean R_{eco} fluxes ranged from 129.0 ± 14.0 mg CO_2-C/m^2/h in the cropland site Priednieki to 190.8 ± 9.0 mg CO_2-C/m^2/h in the grassland site Riebiķi.

Similarly to R_{eco}, statistically significant differences ($P < 0.05$) in R_{het} fluxes (CO_2 fluxes from OM decomposition) were observed not only among different months during the growing season (April to October) within the same study site but also among study sites (Figure 4). Monthly mean R_{het} fluxes ranged from 43.9 ± 3.8 mg CO_2-C/m^2/h in October in the cropland site Priednieki to 229.0 ± 14.1 mg CO_2-C/m^2/h in August in the grassland site Riebiķi. When pooling data from all cropland and grassland sites, significantly higher R_{het} values were observed in grassland sites than in cropland sites in summer months ($P < 0.001$) and in October ($P = 0.006$). Growing season mean R_{het} fluxes ranged from 84.5 ± 8.0 mg CO_2-C/m^2/h in the cropland site Lagzdiņš to 147.0 ± 5.0 mg CO_2-C/m^2/h in the grassland site Riebiķi. Mean proportion of R_{het} from R_{eco} during the growing season was 48.7 ± 2.2% in the grassland sites and 51.5 ± 12.3% in the cropland sites. Furthermore, the proportion of R_{het} within R_{eco} tended to decrease at higher air and consequently soil temperatures (Figure 6).

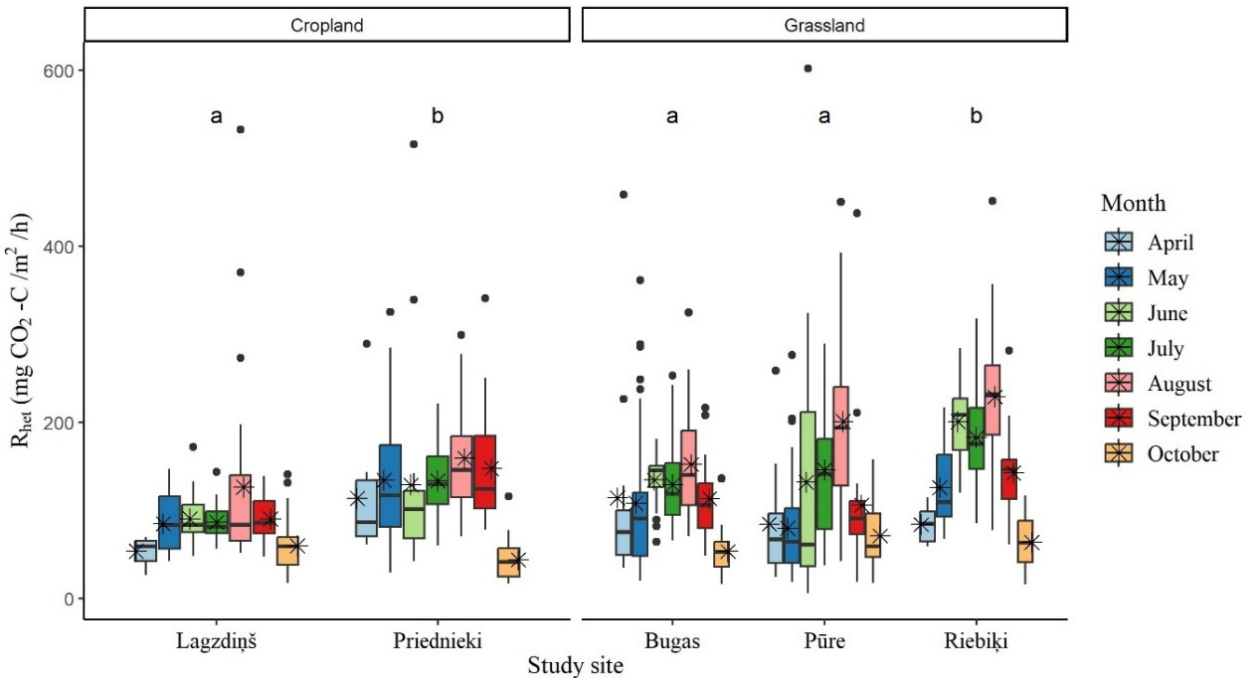

Figure 4. Monthly variation in heterotrophic respiration (R_{het}) (April to October) across different study sites during the growing season. In boxplots, medians are shown as bold horizontal lines in the boxes that indicate the interquartile range from 25th to 75th percentiles, the mean values are shown as black asterisks, and outliers are shown as black dots. Different lowercase letters (a and b) indicate significant differences ($P < 0.05$) between study sites within the same land use type (data pooled from all months)

https://doi.org/10.17221/323/2025-PSE

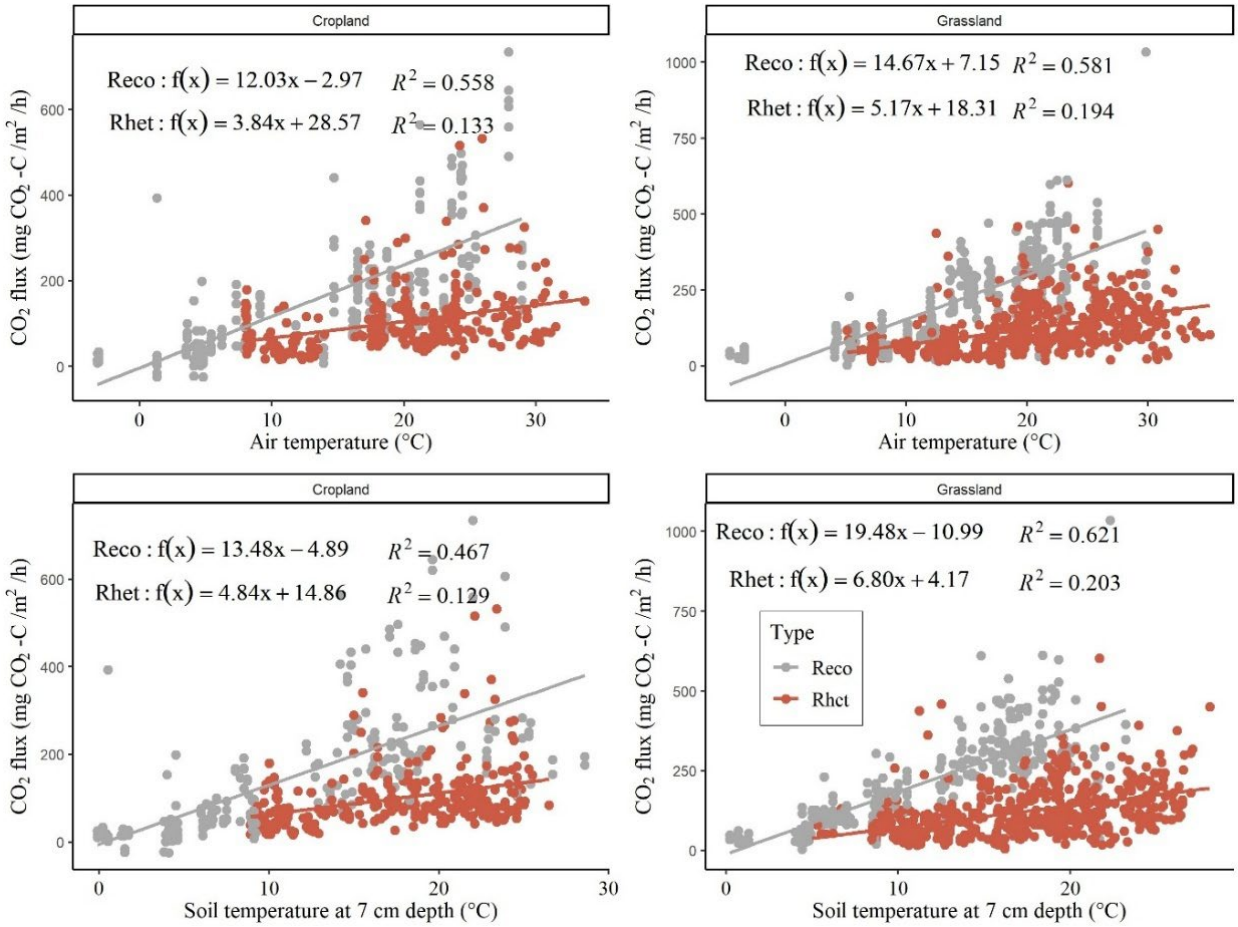

Figure 6. Relationships between instantaneous CO_2 fluxes (ecosystem respiration (R_{eco}) and soil heterotrophic respiration (R_{het})) and air and soil temperature in the grassland and cropland sites

Similarly, Tufekcioglu et al. (2001) in central Iowa (USA) and Lohila et al. (2003) in Finland reported higher soil respiration (CO_2 fluxes) in grassland than in cropland sites, attributing this difference to greater root biomass and higher annual C inputs in perennial grasslands. A similar pattern was observed at our study sites, where a higher amount of live roots in grassland compared with cropland (22.1 ± 2.3 *vs.* 3.8 ± 1.6 t/ha, respectively) likely directly contributed to increased R_{aut}. In addition, the dense rhizosphere in grasslands may promote higher microbial activity, while greater C inputs (6.4 ± 0.7 *vs.* 2.7 ± 0.5 t C/ha, respectively; Table 4) may enhance R_{het} through intensified organic matter decomposition.

Among the study sites and seasons, mean CH_4 fluxes ranged from –52.1 ± 5.9 μg CH_4-C/m^2/h in summer in the grassland site Riebiķi to 60.3 ± 53.8 μg CH_4-C/m^2/h in spring in the cropland site Lagzdiņš. Annual mean CH_4 fluxes ranged from –30.9 ± 8.5 μg CH_4-C/m^2/h in the grassland site Riebiķi (significantly lower CH_4 fluxes indicating net uptake from the atmosphere, $P < 0.001$, Figure 5) to 8.5 ± 6.1 μg CH_4-C/m^2/h in the grassland site Bugas.

Among the study sites and seasons, mean N_2O fluxes ranged from –1.5 ± 6.2 μg N_2O-N/m^2/h in summer in the grassland site Riebiķi to 63.2 ± 29.5 μg N_2O-N/m^2/h in summer in the cropland site Priednieki. No statistically significant differences in N_2O fluxes were observed between different study sites ($P > 0.480$, Figure 5). Annual mean N_2O fluxes were 21.4 ± 4.3 μg N_2O-N/m^2/h in the grassland sites and 25.9 ± 3.1 μg N_2O-N/m^2/h in the cropland sites.

The Spearman correlation analysis between instantaneous GHG fluxes and directly measured environmental variables showed that both R_{eco} and R_{het} were positively correlated with air temperature and soil temperature (Table 5, Figure 6). Although no clear relationships between CO_2 fluxes (R_{eco} and R_{het}) and soil moisture or WTL were found (Table 5), regressions between R_{eco} and soil moisture tended to reflect negative relationship, while regressions between R_{het} and soil moisture tended to reflect

https://doi.org/10.17221/323/2025-PSE

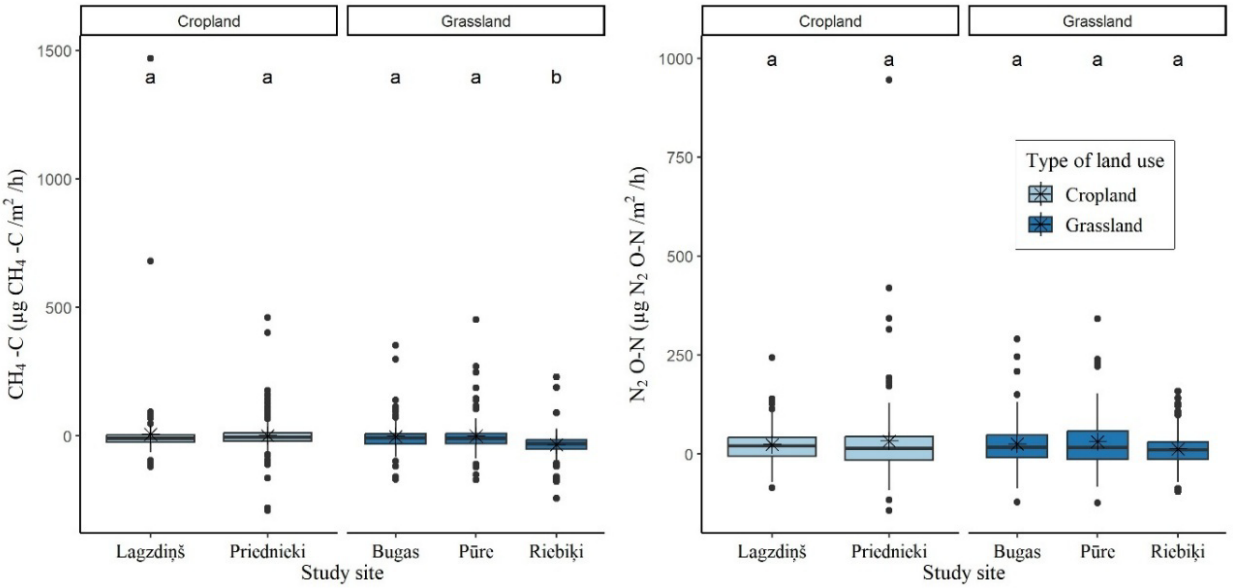

Figure 5. Variation in CH_4 and N_2O fluxes across different study sites during the study period. In boxplots, medians are shown as bold horizontal lines in the boxes that indicate the interquartile range from 25th to 75th percentiles, the mean values are shown as black asterisks, and outliers are shown as black dots. Different lowercase letters (a and b) indicate significant differences ($P < 0.05$) between study sites within the same land use type

downward-opening parabola, which reveal a maximum of R_{het} near 23% soil moisture. At the same time, positive correlations were found between mean R_{eco} and flood frequency ($\rho = 0.66$, $P = 0.007$) and mean flood duration ($\rho = 0.58$, $P = 0.0245$).

The PLS analyses that attempted to explain the variation in instantaneous R_{eco} with the directly and indirectly measured environmental variables resulted in a strong model both for croplands (goodness of fit R^2 was 0.66, goodness of prediction Q^2 was 0.63) and grassland (goodness of fit R^2 was 0.66, goodness of prediction Q^2 was 0.65). The environmental variables that best explained the variation (VIP > 1) were the air temperature and soil temperature, with ETc and SPEI (60-day summary) additionally at cropland sites. The PLS model also included variables with a VIP > 0.8 (soil moisture, FWI and Q (40-day summary) for cropland and ETc, SPEI (60-day summary), FWI and Q (40-day summary) for grassland). The environmental variables that were positively related to the instantaneous R_{eco} were air temperature, soil temperature, ETc and FWI, while the other environmental variables (soil moisture, SPEI, and Q) were related negatively.

Table 5. Spearman's rank correlation coefficients (ρ) between instantaneous greenhouse gas (GHG) fluxes and environmental variables, based on data pooled from all study sites and all calendar months

Variable	Air temperature (°C)	Soil temperature, 7 cm depth (°C)	Soil moisture, 0–7 cm layer (%)	Water-table level* (cm)
Soil temperature, 7 cm depth (°C)	**0.92**			
Soil moisture, 0–7 cm layer (%)	**–0.36**	**–0.41**		
Water-table level* (cm)	**0.27**	**0.27**	**–0.45**	
R_{eco} (mg CO_2-C/m^2/h)	**0.79**	**0.78**	**–0.24**	**0.20**
R_{het} (mg CO_2-C/m^2/h)	**0.50**	**0.47**	0.005	0.12
CH_4-C fluxes (µg CH_4-C/m^2/h)	**–0.31**	**–0.29**	**0.22**	**–0.26**
N_2O-N fluxes (µg N_2O-N/m^2/h)	**0.11**	**0.13**	–0.03	0.08

*Data available only in grassland sites. Statistically significant correlations ($P < 0.05$) are indicated in bold. R_{eco} – ecosystem respiration; R_{het} – heterotrophic respiration

https://doi.org/10.17221/323/2025-PSE

Thus, our results support previous findings across diverse ecosystems that magnitude of CO_2 fluxes is driven largely by air and subsequently soil temperature, which, in combination with soil moisture and related parameters, either directly or indirectly affects vegetation growth and microbial activity in the soil (Almagro et al. 2009, Kochiieru et al. 2023, Walkiewicz et al. 2025). Ansari et al. (2024) based on a comprehensive literature search recently concluded that the wet soil conditions due to the flooding and heavy rainfall events contributed more to the soil CO_2 emission (around 3 g CO_2-C/m^2/day) relative to dry soil conditions (around 2 g CO_2-C/m^2/day) in temperate riparian systems. Also, our results showed higher R_{het} in grassland sites, which experience more frequent flooding than cropland sites. However, higher R_{het} in grassland sites could also be related to differences in spatial distribution of vegetation in general and higher dead OM input with plant biomass and flooding sediments (principal C source to decomposer microorganisms) and subsequent decomposition and CO_2 release.

Only weak correlations were observed between instantaneous CH_4 or N_2O fluxes and directly measured environmental variables (Table 5), and no significant relationships were identified between mean CH_4 or N_2O fluxes and floodplain hydrological regime parameters (Table 3). Also, the PLS analyses using directly and indirectly measured environmental variables resulted in weak models ($R^2 < 0.1$). In general, the magnitude of CH_4 flux is highly dependent on soil moisture status, which may reduce the aerobic zone and thus methanotrophic bacteria activity, while promoting conditions favourable for methanogens (Rey-Sanchez et al. 2019). Ansari et al. (2024) also recently concluded that higher soil CH_4 and N_2O flux in temperate riparian systems was observed from water-saturated soils after flooding events/during wet seasons than from dry soils (12 *vs.* 2.6 mg CH_4-C/m^2/h and 0.7 *vs.* 0.01 mg N_2O-N/m^2/h). Although our grassland sites suffer from flooding periods more often than cropland sites (Table 3), mean annual CH_4 fluxes from alluvial soils in grassland reflected slight removals from the atmosphere, while cropland sites were slight source of CH_4 emissions (Table 4).

No statistically significant correlations were found between plot-level mean GHG fluxes and general physico-chemical variables of soil, excluding negative correlations between mean R_{eco} and soil C/N ratio at 0–10 cm depth ($\rho = -0.63$, $P = 0.014$) and between mean CH_4 fluxes and soil C/N ratio at 10–20 cm depth ($\rho = -0.53$, $P = 0.047$), as well as positive correlations between mean R_{eco} and K content at 40–80 cm depth ($\rho = 0.54$, $P = 0.042$). Obtained correlations reflect the impact of soil OM decomposability and nutrient availability on magnitude of GHG fluxes (Bodelier and Steenbergh 2014, Walkiewicz et al. 2025).

In general, the most important factors influencing N_2O emissions from agricultural soils include the rate and type of nitrogen application (Wallman et al. 2022), with both linear and non-linear increases reported under elevated N inputs (Kim et al. 2013). In this study, no statistically significant differences in N_2O fluxes were observed among the study sites, although mineral fertiliser was applied at one of the cropland sites (Lagzdiņš). This can be explained by the optimal N input with mineral fertiliser application (~130 kg N/ha/year). N surplus appeared to be a more important driver of N_2O emissions than the N application rate itself (Wallman et al. 2022).

Cumulative annual GHG fluxes. Although cumulative annual CH_4 fluxes at the two grassland sites showed slight CH_4 uptake from the atmosphere (negative annual CH_4 flux values), all studied alluvial soils acted as sources of total net GHG emissions (Table 4). Cumulative annual GHG emissions expressed as CO_2 equivalents (eq.) were two times greater in cropland (14.5 ± 4.8 t CO_2 eq./ha/year) than in grassland sites (7.0 ± 3.4 t CO_2 eq./ha/year). Annual net CO_2 emissions (mean 13.6 ± 4.8 and 6.2 ± 3.4 t CO_2/ha/year in cropland and grassland sites, respectively) contributed the most to total net GHG emissions from alluvial soils, ranging from 78% to 94% across study sites. Similarly, Lin et al. (2022) reported significantly higher cumulative CO_2 and N_2O emissions in cultivated wetland (cropland) than those in the other wetland types (riverside and mesophytic wetlands) in the Yellow River floodland, China. Higher total net GHG fluxes, particularly CO_2, in the studied cropland than in grassland sites can be explained by differences in management practices and the resulting conditions. These include ploughing, which enhances soil aeration and thus aerobic soil respiration (CO_2 efflux) by reducing C inputs to the soil from plant residues, particularly dead root biomass. The balance between CO_2 efflux and C input to the soil ultimately determines net soil CO_2 fluxes. Ansari et al. (2004) highlighted that limited information on net C release from riparian systems still hinders assessments of these ecosystems, including C sources and sinks and their contributions to the global climate. However, our study helps to reduce

https://doi.org/10.17221/323/2025-PSE

this knowledge gap by improving understanding of GHG fluxes from agricultural alluvial soils under hemiboreal conditions.

The IPCC guidelines, which serve as a basis for preparing national GHG inventories, do not provide specific GHG emission factors (EFs) for alluvial soils; however, they do provide GHG EFs for flooded land and for drained and rewetted organic soils (IPCC 2006, 2014). In general, cumulative annual net GHG emissions from the studied alluvial soils were substantially lower than those from drained organic soils, but higher than those from flooded soils and similar to those from rewetted organic soils. Estimated cumulative annual net CO_2 emissions, which were the main contributor to total net GHG emissions, from alluvial soils were considerably lower not only than IPCC CO_2 EFs for drained organic soil under agriculture (7.9 t CO_2-C/ha/year in cropland and 6.1 t CO_2-C/ha/year in deep-drained, nutrient-rich grassland in the temperate climate zone; IPCC 2014) but also lower than the annual net CO_2 fluxes recently estimated specifically for drained organic agricultural soils in the hemiboreal region of Europe (4.8 ± 0.8 t CO_2-C/ha/year in cropland and 3.8 ± 0.7 t CO_2-C/ha/year in grassland, Bardule et al. (2025)). A similar effect of soil type on the magnitude of soil respiration in agricultural fields was reported by Lohila et al. (2003) in Finland, who observed that soil respiration rates in peat soils were 2–3 times higher than those in mineral sandy and clay soils. However, the estimated cumulative annual net CO_2 fluxes from the studied alluvial soils were relatively high, considering that these soils did not meet the definition of organic soils (IPCC 2006). This may be related to a potential underestimation of C input into the soil, particularly at grassland sites that were flooded more frequently, during which natural mortality could increase and additional OM could be transported and deposited – processes not included in the net CO_2 flux estimation.

Although the number of study sites is limited, the results support the hypothesis that grassland is a more climate-friendly form of floodplain land use than cropland in the hemiboreal region of Europe, characterised by lower cumulative annual GHG emissions and higher soil C_{org} and N_{tot} stocks. In general, the estimated total GHG emissions, particularly CO_2 emissions, cannot be considered negligible; furthermore, prolonged flooding and soil flooding-drying conditions resulting from heavy precipitation (predicted in several climate change scenarios) can further increase GHG emissions (Guo et al. 2023). Therefore, further research is needed to continue estimating GHG emissions from managed alluvial soils in floodplains, particularly in the context of a changing climate and increasingly frequent extreme weather events.

Acknowledgement. The field measurement data are acquired within the scope of the project "Improving the system for accounting of greenhouse gas (GHG) emissions and carbon dioxide (CO_2) sequestration due to management of arable land and grassland and development of appropriate methodological solutions", Project No. 24-00-S0INZ03-000026. Contribution of Andis Lazdiņš is funded by the PeatTransform project (Research and Innovation Based Solutions to Support the Peat Sector's Transition to a Climate Neutral Economy, No. 6.1.1.2/1/25/A/001).

REFERENCES

Allen R.G., Pereira L.S., Raes D., Smith M. (1998): Crop Evapotranspiration (Guidelines for Computing Crop Water Requirements). Rome, FAO.

Almagro M., López J., Querejeta J.I., Martínez-Mena M. (2009): Temperature dependence of soil CO_2 efflux is strongly modulated by seasonal patterns of moisture availability in a Mediterranean ecosystem. Soil Biology and Biochemistry, 41: 594–605.

Amorim H.C.S., Hurtarte L.C.C., Souza I.F., Zinn Y.L. (2022): C:N ratios of bulk soils and particle-size fractions: global trends and major drivers. Geoderma, 425: 116026.

Ansari J., Bardhan S., Davis M.P., Anderson S.H., Al-Awwal N. (2024): Greenhouse gas emissions from riparian systems as affected by hydrological extremes: a mini-review. Cogent Food and Agriculture, 10: 2321658.

Arcement G.J., Schneider V.R. (1989): Guide for Selecting Manning's Roughness Coefficients for Natural Channels and Floodplains. U.S. Geological Survey Water-Supply Paper 2339. Washington, DC, U.S. Geological Survey: 38.

Bārdule A., Laiho R., Jauhiainen J., Soosaar K., Lazdiņš A., Armolaitis K., Butlers A., Čiuldienė D., Haberl A., Kull A., Muraškienė M., Ostonen I., Rohula-Okunev G., Kamil-Sardar M., Schindler T., Vahter H., Vigricas E., Līcīte I. (2025): Annual net CO_2 fluxes from drained organic soils used for agriculture in the hemiboreal region of Europe. Biogeosciences, 22: 4241–4259.

Bardule A., Lupikis A., Butlers A., Lazdins A. (2017): Organic carbon stock in different types of mineral soils in cropland and grassland in Latvia. Zemdirbyste-Agriculture, 104: 3–8.

Basheer S., Wang X., Farooque A.A., Nawaz R.A., Pang T., Neokye E.O. (2024): A review of greenhouse gas emissions from agricultural soil. Sustainability, 16: 16114789.

https://doi.org/10.17221/323/2025-PSE

Beguería S., Vicente-Serrano S.M., Reig F., Latorre B. (2014): Standardized precipitation evapotranspiration index (SPEI) revisited: parameter fitting, evapotranspiration models, tools, datasets and drought monitoring. International Journal of Climatology, 34: 3001–3023.

Bodelier P.L.E., Steenbergh A.K. (2014): Interactions between methane and the nitrogen cycle in light of climate change. Current Opinion in Environmental Sustainability, 9–10: 26–36.

Boettinger J.L. (2005): Alluvium and alluvial soils. In: Hillel D. (ed.): Encyclopedia of Soils in the Environment. Amsterdam, Elsevier, 45–49. ISBN: 978-0-12-348530-4

Brust G.E. (2019): Management strategies for organic vegetable fertility. In: Biswas D., Micallef S.A. (eds.): Safety and Practice for Organic Food. Amsterdam, Academic Press, 193–212. ISBN: 978-0-12-812060-6

Butlers A., Laiho R., Lazdiņš A., Schindler T., Soosaar K., Jauhiainen J., Bārdule A., Kamil-Sardar M., Līcīte I., Samariks V., Haberl A., Vahter H., Čiuldienė D., Anttila J., Armolaitis K. (2025): Organic soils can be CO_2 sinks in both drained and undrained hemiboreal peatland forests. Biogeosciences, 22: 4627–4647.

Cassell A. (2016): Using R for statistics: a beginner's manual. In: Atanelov L. (ed.): Resident's Handbook of Medical Quality and Safety. Cham, Springer. ISBN: 978-3-030-48067-5

Chataut G., Bhatta B., Joshi D., Subedi K., Kafle K. (2023): Greenhouse gases emission from agricultural soil: a review. Journal of Agriculture and Food Research, 11: 100533.

Donath T.W., Schmiede R., Otte A. (2015): Alluvial grasslands along the northern upper Rhine – nature conservation value *vs.* agricultural value under non-intensive management. Agriculture, Ecosystems and Environment, 200: 102–109.

Dos Santos Pinto R.M., Weigelhofer G., Diaz-Pines E., Brito A.G., Zechmeister-Boltenstern S., Hein T. (2020): River-floodplain restoration and hydrological effects on GHG emissions: biogeochemical dynamics in the parafluvial zone. Science of The Total Environment, 715: 136980.

Dyukarev A.E. (2017): Partitioning of net ecosystem exchange using chamber measurements data from bare soil and vegetated sites. Agricultural and Forest Meteorology, 239: 236–248.

European Union (1992): Consolidated Text: Council Directive 92/43/EEC of 21 May on the Conservation of Natural Habitats and of Wild Fauna and Flora. Official Journal of the European Communities, L206: 7–50.

European Union (2024): Regulation (EU)/1991 of the European Parliament and of the Council of 24 June 2024 on Nature Restoration and Amending Regulation (EU) 2022/869. Official Journal of the European Union, L168: 1–35.

Freeman B.W.J., Evans C.D., Musarika S., Morrison R., Newman T.R., Page S.E., Wiggs G.F.S., Bell N.G.A., Styles D., Wen Y., Chadwick D.R., Jones D.L. (2022): Responsible agriculture must adapt to the wetland character of mid-latitude peatlands. Global Change Biology, 28: 3795–3811.

Guillaume T., Makowski D., Libohova Z., Bragazza L., Sallaku F., Sinaj S. (2022): Soil organic carbon saturation in cropland-grassland systems: storage potential and soil quality. Geoderma, 406: 115529.

Guo Y., Saiz E., Radu A., Sonkusale S., Ullah S. (2023): Prolonged flooding followed by drying increase greenhouse gas emissions differently from soils under grassland and arable land uses. Geoderma Regional, 34: e00697.

IPCC (2006): IPCC Guidelines for National Greenhouse Gas Inventories. In: Eggleston H.S., Buendia L., Miwa K., Ngara T., Tanabe K. (eds.): 2006 IPCC Guidelines for National Greenhouse Gas Inventories. Tokyo, National Greenhouse Gas Inventories Programme, IGES.

IPCC (2014): 2013 Supplement to the 2006 IPCC Guidelines for National Greenhouse Gas Inventories: Wetlands. In: Hiraishi, T., Krug, T., Tanabe, K., Srivastava, N., Baasansuren, J., Fukuda, M., Troxler, T.G. (eds.): 2013 Supplement to the 2006 IPCC Guidelines for National Greenhouse Gas Inventories: Wetlands. Geneva, IPCC.

Jansson J., Hofmockel K. (2019): Soil microbiomes and climate change. Nature Reviews Microbiology, 18: 35–46.

Jian J., Vargas R., Anderson-Teixeira K.J., Stell E., Herrmann V., Horn M., Kholod N., Manzon J., Marchesi R., Paredes D., Bond-Lamberty B.P. (2021): A709 Global Database of Soil Respiration Data, Version 5.0., Oak Ridge, Tennessee.

Kabala C. (2022): Origin, transformation and classification of alluvial soils (mady) in Poland – soils of the year. Soil Science Annual, 73: 156043.

Kim D.G., Hernandez-Ramirez G., Giltrap D. (2013): Linear and nonlinear dependency of direct nitrous oxide emissions on fertilizer nitrogen input: a meta-analysis. Agriculture, Ecosystems and Environment, 168: 53–65.

Kobierski M., Kondratowicz Maciejewska K., Labaz B. (2025): Impact of agricultural land use on organic carbon content in the surface layer of Fluvisols in the Vistula River floodplains, Poland. Agronomy, 15: 628.

Kochiieru M., Veršulienė A., Feiza V., Feizienė D. (2023): Trend for soil CO_2 efflux in grassland and forest land in relation with meteorological conditions and root parameters. Sustainability, 15: 7193.

Kucheryavskiy S. (2020): Mdatools – R package for chemometrics. Chemometrics and Intelligent Laboratory Systems, 198: 103937.

Latvia's National Inventory Report (2025): Available at: https://unfccc.int/ghg-inventories-annex-i-parties/2025 (accessed on 6 November 2025)

LEGMC (2024): Klimata Portals. Available at: https://klimats.meteo.lv/klimats_latvija/latvijas_klimatiskais_raksturojums/ (accessed on 14 November 2024)

LGIA (2025): Basic Data of the Digital Surface Model. Available at: https://www.lgia.gov.lv/en/Digit%C4%81lais%20virsmas%20modelis (accessed on 10 June 2025)

Lin Q., Wang S., Li Y., Riaz L., Yu F., Yang Q., Han S., Ma J. (2022): Effects and mechanisms of land-types conversion on greenhouse

gas emissions in the Yellow river floodplain wetland. Science of The Total Environment, 813: 152406.

Lohila A., Aurela M., Regina K., Laurila T. (2003): Soil and total ecosystem respiration in agricultural fields: effect of soil and crop type. Plant and Soil, 251: 303–317.

Magnusson B., Näykki T., Hovind H., Krysell M., Sahlin E. (2017): Handbook for Calculation of Measurement Uncertainty in Environmental Laboratories, Nordtest Report TR 537, 4th Edition. Taastrup.

Ministry of Agriculture (2019): Digital soil database (INSPIRE data). Riga. Available at: https://inspire geoportal.ec.europa.eu/srv/api/records/%7B122E6F8A-799C-4E94-A61E-6AAC66CEDACE%7D?language=all (accessed on November 15, 2024)

Myhre G., Shindell D., Bréon F.-M., Collins W., Fuglestvedt J., Huang J., Koch D., Lamarque J.-F., Lee D., Mendoza B., Nakajima T., Robock A., Stephens G., Takemura T., Zhang H. (2013): Anthropogenic and natural radiative forcing. In: Stocker T.F., Qin D., Plattner G.-K., Tignor M., Allen S.K., Boschung J., Nauels A., Xia Y., Bex V., Midgley P.M. (eds.): Climate Change: The Physical Science Basis. Contribution of Working Group I to the Fifth Assessment Report of the Intergovernmental Panel on Climate Change. Cambridge, University Press.

Oertel C., Matschullat J., Zurba K., Zimmermann F., Erasmi S. (2016): Greenhouse gas emissions from soils – a review. Chemie Der Erde-Geochemistry, 76: 327–352.

Ojanen P., Minkkinen K., Lohila A., Badorek T., Penttilä T. (2012): Chamber measured soil respiration: a useful tool for estimating the carbon balance of peatland forest soils? Forest Ecology and Management, 277: 132–140.

Palosuo T., Heikkinen J., Regina K. (2015): Method for estimating soil carbon stock changes in Finnish mineral cropland and grassland soils. Carbon Management, 6: 207–220.

Pavelka M., Acosta M., Kiese R., Altimir N., Brümmer C., Crill P., Darenova E., Fuß R., Gielen B., Graf A., Klemedtsson L., Lohila A., Longdoz B., Lindroth A., Nilsson M., Jiménez S.M., Merbold L., Montagnani L., Peichl M., Pihlatie M., Pumpanen J., Ortiz P.S., Silvennoinen H., Skiba U., Vestin P., Weslien P., Janous D., Kutsch W. (2018): Standardisation of chamber technique for CO_2, N_2O and CH_4 fluxes measurements from terrestrial ecosystems. International Agrophysics, 32: 569–587.

Petaja G., Ivbule I., Zvaigzne Z.A., Purviņa D., Upenieks E.M., Līcīte I., Lazdiņš A. (2024): Organic carbon stock in mineral soils in cropland and grassland in Latvia. Environments, 11: 73.

Petsch D.K., de Mello Cionek V., Thomaz S.M., Carneiro N., dos Santos L. (2023): Ecosystem services provided by river-floodplain ecosystems. Hydrobiologia, 850: 2563–2584.

R Core Team: The R Project for Statistical Computing. Available at: https://www.R-project.org (accessed on 14 November 2024)

Rey-Sanchez C., Bohrer G., Slater J., Li Y.-F., Grau-Andrés R., Hao Y., Rich V.I., Davies G.M. (2019): The ratio of methanogens to methanotrophs and water-level dynamics drive methane transfer velocity in a temperate kettle-hole peat bog. Biogeosciences, 16: 3207–3231.

Schweizer S.A., Mueller C.W., Höschen C., Ivanov P., Kögel-Knabner I. (2021): The role of clay content and mineral surface area for soil organic carbon storage in an arable toposequence. Biogeochemistry, 156: 401–420.

Šeffer J., Janák M., Šefferová Stanová V. (2008): Management models for habitats in Natura Sites: 6440 Alluvial meadows of river valleys of the Cnidion dubii. European Commission.

Tabari H. (2020): Climate change impact on flood and extreme precipitation increases with water availability. Scientific Reports, 10: 13768.

Thorp J. (1968): Alluvium. In: Geomorphology. Encyclopedia of Earth Science; Berlin, Heidelberg, Springer.

Tripolskaja L., Toleikiene M., Skersiene A., Versuliene A. (2024): Biomass of shoots and roots of multicomponent grasslands and their impact on soil carbon accumulation in Arenosol rich in stones. Land, 13: 1098.

Tufekcioglu A., Raich J., Isenhart T., Schultz R.C. (2001): Soil respiration within riparian buffers and adjacent crop fields. Plant and Soil, 229: 117–124.

Van Eekeren N., Dekker J., Geerts R., Janssen P., Stip A., Visser T., Bloem J., de Goede R. (2025): Disturbance from tillage is a dominant factor in explaining differences in soil biodiversity of three grasslands management types. Applied Soil Ecology, 206: 105881.

Van Wagner C.E. (1987): Development and structure of the Canadian Forest Fire Weather Index System. Forestry Technical Report. 35. Chalk River, ON: Canadian Forest Service, Petawawa National Forestry Institute.

Vicente-Serrano S.M., Beguería S., López-Moreno J.I. (2010): A multiscalar drought index sensitive to global warming: the standardized precipitation evapotranspiration index. Journal of Climate, 23: 1696–1718.

Walkiewicz A., Bulak P., Khalil M.I., Osborne B. (2025): Assessment of soil CO_2, CH_4, and N_2O fluxes and their drivers, and their contribution to the climate change mitigation potential of forest soils in the Lublin region of Poland. European Journal of Forest Research, 144: 29–52.

Wallman M., Lammirato C., Delin S., Klemedtsson L., Weslien P., Rütting T. (2022): Nitrous oxide emissions from five fertilizer treatments during one year – high-frequency measurements on a Swedish Cambisol. Agriculture, Ecosystems and Environment, 337: 108062.

Wang X., Wotton B.M., Cantin A., Parisien M.A., Anderson K., Moore B., Schiks T., Flannigan M.D. (2025): *cffdrs*: Canadian Forest Fire Danger Rating System (R package version 1.9.2). doi: 10.32614/CRAN.package.cffdrs

Received: July 21, 2025
Accepted: March 9, 2026
Published online: March 25, 2026